Constraining $t \to u$ flavor changing neutral Higgs coupling at the LHC

Wei-Shu Hou, Ting-Hsiang Hsu and Tanmoy Modak
Department of Physics, National Taiwan University, Taipei 10617, Taiwan

We study the constraints on $t \to u$ flavor changing neutral Higgs (FCNH) coupling, and how it may be explored further at the Large Hadron Collider (LHC). In the general two Higgs doublet model, such transitions can be induced by a nonzero ρ_{tu} Yukawa coupling. We show that such couplings can be constrained by existing searches at the LHC for m_H, m_A and, m_{H^+} in the sub-TeV range, where H, A and H^+ are the exotic CP-even, CP-odd and charged scalars. We find that a dedicated $ug \to tH/tA \to tt\bar{u}$ search can probe the available parameter space of ρ_{tu} down to a few percent level for $200\,\text{GeV} \lesssim m_H,\, m_A \lesssim 600$ GeV, with discovery possible at high luminosity. Effects of how other extra top Yukawa couplings, such as ρ_{tc} and ρ_{tt}, dilute the sensitivity of the ρ_{tu} probe are discussed.

arXiv:2008.02573v1 [hep-ph] 6 Aug 2020

I. INTRODUCTION

The 125 GeV scalar boson h, only discovered [1] in 2012, combines with the longitudinal components of the massive vector bosons to form the weak scalar doublet of the Standard Model (SM). But with one scalar doublet established naturally brings in the question of a second doublet, i.e. the so-called [2] two Higgs doublet model (2HDM). Although it is popular [2] to use a discrete symmetry to impose "Natural Flavor Conservation" [3] so all "dangerous" flavor changing neutral Higgs (FCNH) couplings are removed, it is also well known that this may not be necessary [2]. Indeed, upon the discovery of h, the $t \to ch$ decay [4] search was advocated [5] and quickly pursued by ATLAS [6] at the LHC, and further efforts are recorded [7] by the Particle Data Group (PDG). As another example, CMS saw early on with 8 TeV data some hint [8] for $h \to \tau\mu$ decay. Though it subsequently disappeared [7], it did bring about considerable interest in FCNH couplings.

As elucidated in Ref. [5], the $t \to ch$ decay occurs via the $c_\gamma \rho_{tc}$ coupling, where $c_\gamma \equiv \cos\gamma$ is the mixing angle of h with the CP-even scalar boson H of the exotic doublet, which is the one that carries the FCNH ρ_{tc} coupling. With subsequent Higgs property studies [9–11], it became clear that h resembles very closely the Higgs boson of SM, and the h–H mixing angle c_γ seems rather small. This may be the reason behind the non-observation [7] of $t \to ch$ so far, without implying ρ_{tc} to be small. Demonstrating [12] that there is quite some parameter space for c_γ to be small in the 2HDM context, it was advocated that mass-mixing hierarchy suppression [4] of FCNH couplings involving lighter generation fermions, augmented by the smallness of c_γ ("alignment"), can explain the absence of low energy FCNH effects without the need to invoke NFC. Thus, extra Yukawa couplings are rather general in the 2HDM setting and should be pursued experimentally, and not just at the LHC. The "Model III" of Ref. [4] was therefore elevated to the general 2HDM (g2HDM), even promoted [13] as a possible future "SM2", the SM with two Higgs doublets.

Having introduced the g2HDM, we write down the couplings of the CP-even scalars h, H and CP-odd scalar A to fermions as [5, 12, 14]

$$\mathcal{L} = -\frac{1}{\sqrt{2}} \sum_{f=u,d,\ell} \bar{f}_i \Big[(-\lambda^f_{ij} s_\gamma + \rho^f_{ij} c_\gamma) h + (\lambda^f_{ij} c_\gamma + \rho^f_{ij} s_\gamma) H - i\,\mathrm{sgn}(Q_f) \rho^f_{ij} A \Big] R\, f_j + \text{H.c.}, \quad (1)$$

where $L, R \equiv (1 \mp \gamma_5)/2$, $i, j = 1, 2, 3$ are generation indices and summed over, $c_\gamma = \cos\gamma$ and $s_\gamma = \sin\gamma$, and u, d, ℓ are up and down type quarks and charged leptons, respectively. The matrices $\lambda^f_{ij} \equiv \sqrt{2} m^f_i \delta_{ij}/v$ are the usual Yukawa couplings related to mass in SM, whereas ρ^f_{ij} are in general non-diagonal and complex. We do not consider H^+ effects in this work, but consider ρ_{tu}-induced processes at the LHC, including $ug \to tH/tA$ production (see Fig. 1). We refrain from quoting the Higgs potential for g2HDM here. Instead, we treat the scalar boson masses as parameters, but state that we have checked that they satisfy the usual requirements of perturbativity, positivity and unitarity, as well as other constraints such as electroweak oblique parameters (see e.g. Refs. [15–17]).

In the experimental pursuit of $t \to ch$, one actually searches for $t \to ch$, uh simultaneously. It turns out that the bound on $t \to uh$ is not better than $t \to ch$, i.e. the current 95% C.L. bound from ATLAS [18] gives

$$\mathcal{B}(t \to uh) < 1.2 \times 10^{-3}, \;\; \mathcal{B}(t \to ch) < 1.1 \times 10^{-3}, \quad (2)$$

based on $36.1\,\text{fb}^{-1}$ data at 13 TeV, which is better than the CMS result [19] based on similar amount of data. This may seem surprising since single top production via ρ_{tu} is taken into account. One may think that ρ_{tu} should naturally be much smaller than ρ_{tc}, but this is not based

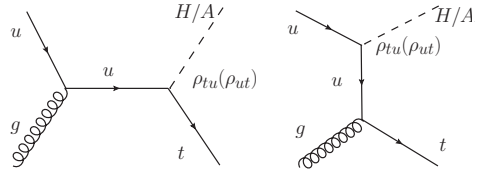


FIG. 1. Feynman diagrams for $ug \to tH/tA$.

on our current experimental knowledge. It was pointed out [20] that $B \to \mu\bar{\nu}$ decay probes the $\rho_{tu}\rho_{\tau\mu}$ product. The process will be pursued by Belle II [21], where a deviation of the ratio $\mathcal{R}_B^{\mu/\tau} = \mathcal{B}(B \to \mu\bar{\nu})/\mathcal{B}(B \to \tau\bar{\nu})$ from the SM expectation of 0.0045 would indicate [20] nonzero ρ_{tu} in g2HDM. What can LHC do to check $\rho_{tu} \neq 0$? In this paper we focus on $ug \to tH/tA \to tt\bar{u}$ production, i.e. $ug \to tH/tA$ (see Fig. 1) followed by $H/A \to t\bar{u}$, leading to same-sign top signature.

In the next section we first summarize the constraint on ρ_{tu} from searches at the LHC, including $t\bar{t}t\bar{t}$ search. We turn to $ug \to tH/tA \to tt\bar{u}$ (conjugate process always implied unless specified) in Sec. III and use it to constrain or discover the ρ_{tu} coupling [22]. We focus on $m_A, m_H \in (200, 600)$ GeV, which is allowed in g2HDM [15–17]. Heavier m_A, m_H are possible, but discovery prospect is reduced due to rapid fall off in parton luminosities. As the ρ_{tc}-induced $cg \to tH/tA \to tt\bar{c}$ process [23–26] (see also Refs. [27–30]) can be misidentified as $ug \to tH/tA \to tt\bar{u}$ due to inefficient c-jet tagging, we outline a procedure to distinguish between the two processes. We comment briefly on the effect of the diagonal ρ_{tt} coupling in Sec. IV, before offering our conclusion.

II. CURRENT CONSTRAINTS ON ρ_{tu}

As stated, our actual knowledge of the strength of ρ_{tu} is actually quite poor.

The h boson couples to tu as $c_\gamma\rho_{tu}$, hence $\mathcal{B}(t \to uh)$ search constrains ρ_{tu} coupling for finite c_γ. The latest ATLAS result based on 36.1 fb^{-1} data at 13 TeV sets the 95% C.L. limit $\mathcal{B}(t \to uh) < 1.1 \times 10^{-3}$ [18], as given in Eq. (2), which is better than the CMS limit [19] of $\mathcal{B}(t \to uh) < 4.7 \times 10^{-3}$ based on 35.9 fb^{-1}. We illustrate the ATLAS limit [18] in Fig. 2 as the blue shaded region in the c_γ–ρ_{tu} plane, while the weaker CMS limit is not displayed. Taking $c_\gamma = 0.2$ as example, one gets $|\rho_{tu}| \lesssim 0.5$ at 95% C.L., which is rather weak, and weakens further for smaller c_γ.

Stronger constraints on ρ_{tu} arise from the $t\bar{t}t\bar{t}$, or $4t$ search, which does not depend on c_γ. Let us first focus on the CMS $4t$ search, which is based on 137 fb^{-1} at 13 TeV, i.e. with full Run 2 data [31], more than three times the data size of the preceding study [32]. Depending on the number of charged leptons (e, μ) and b-tagged jets, the search in Ref. [31] is divided into several signal regions (SRs) and two control regions (CRs), with the baseline selection criterion of at least two same-sign leptons. We find that the most stringent constraint on ρ_{tu} arises from the control region of $t\bar{t}W$, which is denoted as CRW [31]. Induced by the ρ_{tu} coupling, the $ug \to tH/tA \to tt\bar{u}$ process would contribute to this CRW.

CRW of the CMS $4t$ search [31] is defined as containing two same-sign leptons plus two to five jets with two b-tagged. The selection cuts are as follows. Leading (subleading) lepton transverse momentum should satisfy $p_T > 25\,(20)$ GeV. The pseudorapidity of electrons

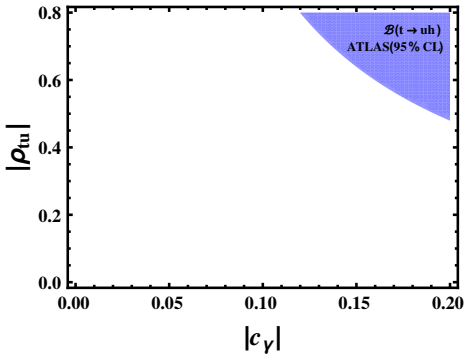


FIG. 2. $\mathcal{B}(t \to uh)$ constraint in $|c_\gamma|$–$|\rho_{tu}|$ plane.

(muons) should satisfy $|\eta| < 2.5\,(2.4)$, while all jets satisfy $|\eta| < 2.4$. The events are selected if p_T of (b-)jets satisfy any of the following three conditions [33]: (i) both b-jets satisfy $p_T > 40$ GeV; (ii) one b-jet with $p_T > 20$ GeV and $20 < p_T < 40$ GeV for the second b-jet, with $p_T > 40$ GeV for the third jet; (iii) both b-jets satisfy $20 < p_T < 40$ GeV, with two extra jets each satisfying $p_T > 40$ GeV. H_T, defined as the scalar sum of p_T of all jets, should satisfy $H_T > 300$ GeV, while $p_T^{\rm miss} > 50$ GeV. To reduce the Drell-Yan background with a charge-misidentified electron, events with same-sign electron pairs with $m_{ee} < 12$ GeV are rejected. With these selection cuts, CMS reports 338 observed events in CRW, while the expected total number of events (SM backgrounds plus $4t$) is at 335 ± 18 [31].

To calculate our limits, we generate signal events using MadGraph5_aMC@NLO [34] (denoted as MadGraph5_aMC) at leading order (LO) with default parton distribution function (PDF) set NN23LO1 [35], interface with PYTHIA 6.4 [36] for showering and hadronization, and MLM matching [37] prescription for matrix element and parton shower merging. The event samples are then fed into Delphes 3.4.2 [38] for fast detector simulation, where we follow the CMS-based detector analysis for CRW, utilize the default b-tagging efficiency and light-jet rejection, with jets reconstructed via anti-k_T algorithm. The effective model is implemented in FeynRules [39].

The ρ_{tu}-induced process $pp \to tH/tA \to tt\bar{u}$ (non-resonant $ug \to tt\bar{u}$ and t-channel H/A exchange $uu \to tt$ processes are included) with both top quarks decaying semileptonically contributes to CRW of CMS $4t$ search. Setting all other $\rho_{ij} = 0$, we estimate the contribution for $\rho_{tu} = 1$ and then scale the cross section by $|\rho_{tu}|^2$, assuming narrow H/A widths with $\mathcal{B}(H/A \to t\bar{u}) = 50\%$. We then demand that the sum of the number of events expected from SM and those from ρ_{tu}-induced processes agree with the observed number of events within 2σ uncertainty of expectations. We display the 2σ exclusion limits obtained via CRW in Fig. 3 as the purple shaded regions, where we assume Gaussian behavior for simplicity. That is, we simplify and do not follow the more precise estimation [40] of exclusion limits using likelihood function with Poisson counting.

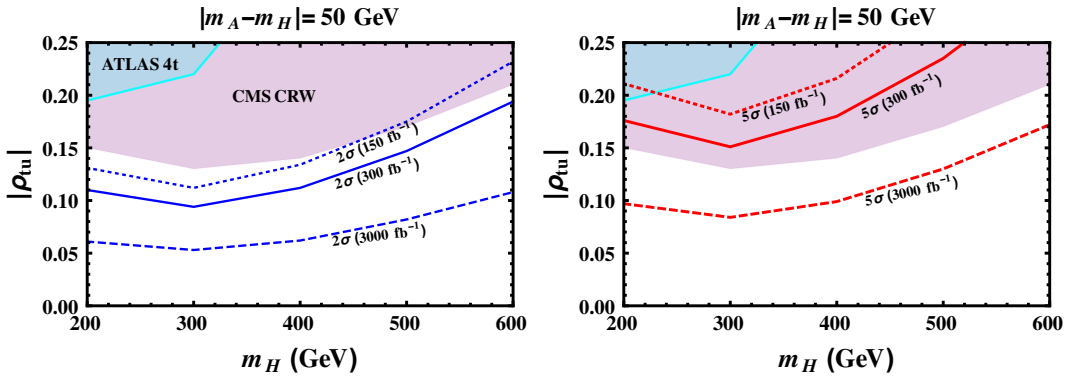


FIG. 3. Exclusion limits [left] and discovery reaches [right] for $|\rho_{tu}|$ by the same-sign top signature with various integrated luminosities at the 14 TeV LHC, where the purple and cyan regions are excluded respectively by CMS CRW [31] and ATLAS CRttW2ℓ [41] control regions. See text for details.

ATLAS has also searched for $4t$ production [41] with 139 fb^{-1}, but categorizing into different SRs and CRs. Again, the CR for $t\bar{t}W$, called CRttW2ℓ, is the most relevant. It is defined as at least two same-sign leptons ($e^\pm\mu^\pm$ or $\mu^\pm\mu^\pm$), plus at least four jets with at least two b-tagged. The same-sign leptons are required to have $p_T > 28$ GeV with $|\eta^\mu| < 2.5$ and $|\eta^e| < 1.5$. All jets should satisfy $p_T > 25$ GeV and $|\eta| < 2.5$. If the number of b-jets is equal to two, or the number of b-jets is ≥ 3 but with no more than 5 jets, the scalar p_T sum over all jets and same-sign leptons (note the difference in definition from CMS), H_T, should satisfy $H_T < 500$ GeV. Unlike CRW for CMS, ATLAS does not give the observed number of events in CRttW2ℓ, but provides a figure of comparison between data and prediction in the variable $\sum p_T^\ell$ (see Ref. [41] for definition). We extract [42] from this figure the number of expected and observed events for CRttW2ℓ, finding 378 ± 10 and 380, respectively, where we have simply added the errors in quadrature for the expected events from each $\sum p_T^\ell$ bin.

To extract the constraint, we follow the same event selection procedure as before, but use the ATLAS-based detector card of Delphes. Assuming that the number of events for $pp \to tH/tA \to tt\bar{u}$ plus SM stay within 2σ of the expected number of events, we illustrate the exclusion limits from ATLAS CRttW2ℓ by the cyan shaded regions in Fig. 3. Mainly due to differences in selection cuts, the ATLAS constraint on ρ_{tu} is weaker. From CMS $4t$ search we find $\rho_{tu} \lesssim 0.13$–0.15 is still allowed for $200\,\text{GeV} \lesssim m_H \lesssim 400$ GeV, while slightly larger values open up for $m_H > 400$ GeV. In this vein, we stress that we have illustrated for $|m_H - m_A| = 50$ GeV, as there is strong cancellation between $ug \to tH \to tt\bar{c}$ and $ug \to tA \to tt\bar{c}$ amplitudes for H, A that are nearly degenerate in mass and width.

We remark that supersymmetry search in similar event topologies can in principle constrain ρ_{tu}. However, such analyses now typically require H_T and/or missing energy that are too large for our purpose. The selection criteria could be relaxed with R-parity violation, e.g. the ATLAS search [43] for squark pair production, but the selection cuts are still too strong to give meaningful constraint. We note further that the ATLAS search for new phenomena in events [44] with same-sign dileptons and b-jets (36.1 fb^{-1} at 13 TeV) has similar SRs, but the cuts are again strong and the selection criteria different, such that it does not give relevant constraint for our study.

III. SAME-SIGN TOP SIGNATURE FROM ρ_{tu}

Even though the existing CMS $4t$ search with full LHC Run 2 data can set meaningful constraints on ρ_{tu}, it is not optimized for $ug \to tH/tA \to tt\bar{u}$ search. In this section, we perform a dedicated study of the $ug \to tH/tA \to tt\bar{u}$ process at the LHC, targeting exclusion or discovery of a stand-alone ρ_{tu} coupling.

A. Discovery and Exclusion Limits

The $pp \to tH/tA + X \to tt\bar{u} + X$ process can be searched for in events containing same-sign dilepton (ee, $\mu\mu$, $e\mu$), at least three jets with at least two b-tagged and one non-b-tagged jet, plus $E_T^{\rm miss}$, which we denote as same-sign top. The final state topology will also receive contribution from $uu \to tt$ via t-channel A/H exchange which we include as signal. The dominant backgrounds are $t\bar{t}Z$, $t\bar{t}W$, $4t$ and $t\bar{t}h$, while $3t{+}W$, $3t{+}j$ and $tZ{+}$jets are subdominant. In addition, if the lepton charge gets misidentified (charge- or Q-flip), with the misidentification efficiency at 2.2×10^{-5} [44–46], the $t\bar{t}{+}$jets and $Z/\gamma^*{+}$jets processes would also contribute. We remark that the CMS study [47] with similar final state topology but with slightly different cuts finds the "nonprompt" backgrounds at ~ 1.5 times the $t\bar{t}W$ background, which is significant. As the nonprompt backgrounds are not properly modeled in Monte Carlo simulations, we simply add this component to the overall background at 1.5 times the $t\bar{t}W$ background after selection cuts.

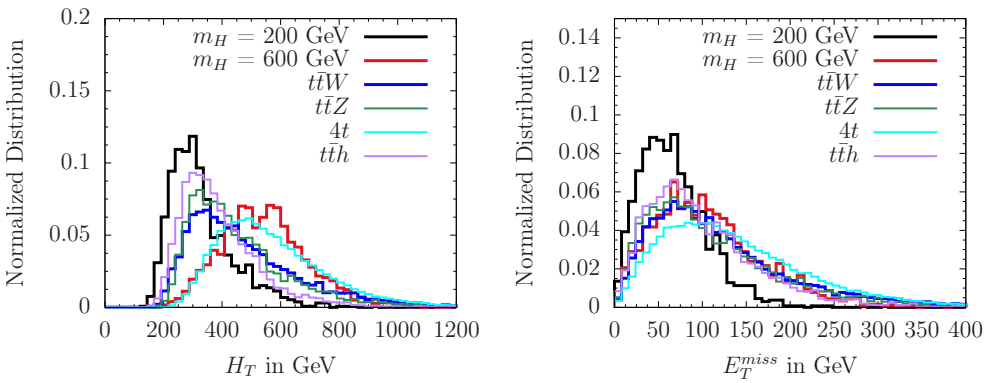


FIG. 4. The normalized H_T (left) and $E_T^{\rm miss}$ (right) distributions for the signal and leading backgrounds. See text for details.

We generate signal and background events as in the previous section at LO via MadGraph5_aMC for $\sqrt{s} = 14$ TeV, follow the same showering, hadronization and ME, and parton shower merging and matching. We adopt here the default ATLAS-based detector card of Delphes. The LO $t\bar{t}W^-$ ($t\bar{t}W^+$), $t\bar{t}Z$, $4t$, $t\bar{t}h$ and, $tZ+$jets cross sections are normalized to next-to-leading order K factors 1.35 (1.27) [48], 2.04 [34], 1.44 [34], 1.27 [49], and 1.56 [50], respectively. We assume the same K factor for $\bar{t}Z+$jets background for simplicity. The Q-flip Z/γ^*+jets and $t\bar{t}+$jets backgrounds are corrected to next-to-next-to-leading (NNLO) order cross sections by 1.27 [51] and 1.84 [52], respectively. We utilize FEWZ 3.1 [53] to obtain the NNLO factor for Z/γ^*+jets background. The signal cross sections and $3t + W$, $3t + j$ backgrounds are kept at LO.

To reduce backgrounds, we follow a cut based analysis that is different from CRW of CMS $4t$ search, and optimize for $pp \to tA/tH + X \to tt\bar{u} + X$ as follows. The leading (subleading) lepton should have $p_T > 25$ (20) GeV, while $|\eta| < 2.5$ for both leptons. All three jets should satisfy $p_T > 20$ GeV and $|\eta| < 2.5$. The missing energy in each event should satisfy $E_T^{\rm miss} > 30$ GeV. The separation ΔR between a lepton and any jets ($\Delta R_{\ell j}$), between the two b-jets (ΔR_{bb}), and between any two leptons ($\Delta R_{\ell\ell}$) should all satisfy $\Delta R > 0.4$. We finally demand that selected events should satisfy $H_T > 300$ GeV, where H_T is defined according to ATLAS,i.e. including the p_T of the two leading leptons.

We plot in Fig. 4 the normalized H_T and $E_T^{\rm miss}$ distributions before selection cuts for signal and dominant backgrounds. For signal we choose the two representative $m_H = 200$ and 600 GeV values (with $m_A = m_H + 50$ GeV) for illustration. The signal cross section for different m_H with $|m_A - m_H| = 50$ GeV and background cross sections after the selection cuts are summarized in Tables I and II, respectively. We have assumed m_H to be lighter than m_A.

To estimate the exclusion limit (2σ) and discovery potential (5σ), we utilize the test statistics [40]

$$Z(x|n) = \sqrt{-2\ln\frac{L(x|n)}{L(n|n)}}, \qquad (3)$$

where $L(x|n) = e^{-x}x^n/n!$ is the likelihood function of Poisson probabilities with n the observed number of events, and x is either the number of events predicted by the background-only hypothesis b, or signal plus background hypothesis $s+b$. For exclusion ($s+b$ hypothesis) we demand $Z(s+b|b) \geq 2$ for 2σ, while for discovery (b hypothesis) $Z(b|s+b) \geq 5$ for 5σ. Utilizing the signal cross sections for the reference $\rho_{tu} = 1$ value in Table I and the background cross sections in Table II, we find the exclusion and discovery contours in m_H–ρ_{tu} plane (with $m_A = m_H + 50$ GeV) for different integrated luminosities in the left and right panels of Fig. 3, respectively, where we have interpolated the contours for m_H values other than the ones given in Table I for simplicity.

The exclusion and discovery contours are plotted in

m_H [Γ_H] (GeV)	m_A [Γ_H] (GeV)	cross section (fb)
200 [0.81]	250 [4.14]	18.9
300 [8.07]	350 [12.0]	25.6
400 [15.7]	450 [19.6]	18.1
500 [23.2]	500 [26.7]	10.6
600 [30.2]	650 [33.6]	6.0

TABLE I. Mass and width of H and A for $\rho_{tu} = 1$, and same-sign top signal cross section at 14 TeV after selection cuts.

backgrounds	cross section (fb)
$t\bar{t}W$	1.31
$t\bar{t}Z$	0.264
$4t$	0.092
$t\bar{t}h$	0.058
Q-flip	0.024
$tZ+$jets	0.007
$3t + W$	0.001
$3t + j$	0.0004

TABLE II. Background cross sections after selection cuts.

Fig. 3 as blue and red lines, respectively, for the three different integrated luminosities of 150 (dotted), 300 (solid) and 3000 fb^{-1} (dashed). The 150 fb^{-1} data size reflects the target luminosity for Run 2, but the contours are generated with $\sqrt{s} = 14$ TeV rather than 13 TeV. We find that, with 150 (300) fb^{-1} one could exclude $|\rho_{tu}| \gtrsim 0.13$ (0.11) if 200 GeV $\lesssim m_H \lesssim$ 400 GeV, whereas $|\rho_{tu}| \gtrsim$ 0.18–0.25 (0.15–0.19) for 400 GeV $\lesssim m_H \lesssim$ 600 GeV. With full High Luminosity LHC (HL-LHC) data, i.e. with 3000 fb^{-1}, the exclusion limit can reach down to $|\rho_{tu}| \gtrsim 0.06$ for $m_H \lesssim 400$ GeV, and $|\rho_{tu}| \gtrsim 0.1$ for 400 GeV $\lesssim m_H \lesssim$ 600 GeV. One would need larger $|\rho_{tu}|$ for discovery. For example, the discovery contours for 150 and 300 fb^{-1} lie in the regions excluded by CMS CRW. For the HL-LHC dataset, $|\rho_{tu}| \sim 0.1$ (0.17) would be sufficient for discovery for 200 GeV $\lesssim m_H \lesssim$ 400 GeV (400 GeV $\lesssim m_H \lesssim$ 600 GeV).

B. Distinguishing ρ_{tu} and ρ_{tc} Effects

Unless the final state charm can be efficiently tagged (which is not the case), the $cg \to tH/tA \to tt\bar{c}$ processes also give rise to the same-sign top signature for nonzero ρ_{tc}. In this subsection, we outline a procedure to distinguish same-sign top signatures induced by ρ_{tu} vs ρ_{tc}.

The valence u-quark induced $ug \to tH/tA \to tt\bar{u}$ process has much larger cross section compared to $\bar{u}g \to \bar{t}H/\bar{t}A \to \bar{t}\bar{t}u$. So one expects the former to be considerably larger than the latter. To understand the relative significance of $ug \to tH/tA \to tt\bar{u}$, we take a benchmark point with $\rho_{tu} = 0.13$, m_H, $m_A = 300$, 350 GeV that is still allowed by Fig. 3. To distinguish between the signature induced by ρ_{tu} vs ρ_{tc}, we separate positively charged vs negatively charged same-sign dileptons. Following the same analysis as in the previous subsection, we find the signal (background) cross sections at $\sqrt{s} = 14$ TeV for the $++$ and $--$ charged dileptons to be 0.5 fb and 0.06 fb (~ 2.35 fb and ~ 1.38 fb), respectively. We then find the significance for dileptons with $++$ charge to be $\sim 4.1\sigma$ ($\sim 13\sigma$) with 300 (3000) fb^{-1}, while the corresponding significance for $--$ charged dileptons is at $\sim 1\sigma$ ($\sim 2.7\sigma$). Note that the former (latter) arises from the $ug \to tH/tA \to tt\bar{u}$ ($\bar{u}g \to tH/tA \to tt\bar{u}$) process. Thus, separating the $++$ from $--$ same-sign dilepton events, one expects the $++$ dileptons to emerge earlier than the $--$. We have again assumed the non-prompt background to be ~ 1.5 times the $t\bar{t}W$ background, while Q-flip background is assumed at half the value given in Table II for the respective signatures.

In comparison, the c-quark induced $cg \to tH/tA \to tt\bar{c}$ and $\bar{c}$-quark induced $\bar{c}g \to \bar{t}H/\bar{t}A \to \bar{t}\bar{t}c$ processes should have similar cross sections. Assuming all $\rho_{ij} = 0$ except ρ_{tc} we find, for example, that $\rho_{tc} = 0.36$ is allowed at 2σ by CRW of CMS $4t$ search for m_H, $m_A = 300$, 350 GeV. Following the same cut based analysis for these parameter values, we find the cross sections at $\sqrt{s} = 14$ TeV for $++$ and $--$ charged dilepton processes at 0.074 and 0.081 fb, respectively, which translates to $\sim 2.7\sigma$ ($\sim 8.4\sigma$) and $\sim 3.8\sigma$ ($\sim 11.9\sigma$) with 300 (3000) fb^{-1} integrated luminosity. That is, both $++$ and $--$ same-sign dilepton events are at similar level, which contrasts with the ρ_{tu}-induced same-sign dilepton events.

So far we have discussed scenarios when either ρ_{tu} or ρ_{tc} is nonzero. Recasting the results from Ref. [54], it was found [55] that $|\rho^*_{tu}\rho_{tc}| \gtrsim 0.02$ is excluded by D–$\overline{D}$ mixing for $m_H \approx m_A \approx m_{H^\pm} \simeq 500$ GeV, which would be even more stringent for lighter exotic scalars. This gives the ballpark of the constraint when both ρ_{tu} and ρ_{tc} are nonzero. A detailed analysis treating both ρ_{tu} and ρ_{tc} nonzero would be studied elsewhere.

IV. DISCUSSION AND OUTLOOK

Let us comment on the impact of turning on ρ_{tt}. As $\rho_{tt} \neq 0$ would induce $H/A \to t\bar{t}$ decays, the $4t$ search constraints from CRW of CMS and CRttW2ℓ of ATLAS would weaken for $m_H\,(m_A) > 2m_t$ due to $\mathcal{B}(H/A \to t\bar{t}) \neq 0$. In particular, $\rho_{tt} = 0.5$ is still allowed for m_H, m_A, $m_{H^\pm} \sim$ 200–600 GeV [17]. For $\rho_{tu} = 0.15$ and $\rho_{tt} = 0.5$, $\mathcal{B}(H/A \to t\bar{u} + \bar{t}u)$ would be suppressed by $\sim 70\%$–90% for 400 GeV $\lesssim m_H \lesssim$ 600 GeV, weakening the limits from CRW of CMS $4t$ search. Nonzero ρ_{tu} and ρ_{tt} may also induce $ug \to tH/tA \to tt\bar{t}$ (triple-top) and $ug \to bH^+ \to bt\bar{b}$ signatures, where the latter process may even emerge from Run 2 data [17]. Such final states can also arise from ρ_{tc} coupling. However, separating $++$ and $--$ same-sign dileptons can in principle differentiate between ρ_{tu} and ρ_{tc} couplings. Scenarios when ρ_{tu}, ρ_{tc} and ρ_{tt} are all nonzero would receive multiple constraints, in particular from flavor physics. A study involving all three couplings is beyond the scope of this work. However, based on the extensive work on ug, $cg \to tH/tA \to tt\bar{u}$, $tt\bar{c}$, $tt\bar{t}$ processes reported or cited here, we advertise a public twiki page [56] where interested LHC workers could use to join the quest.

At this point, it is useful to recall that ρ_{tt} provides a robust driver [57] for electroweak baryogenesis (EWBG) in g2HDM, even for $|\rho_{tt}|$ values at the percent level, which provides strong motivation. If ρ_{tt} is sizable, it would make probing nonzero ρ_{tu} more challenging at the LHC. However, we have emphasized our current experimental knowledge, and such knowledge on ρ_{tu} comes primarily from the LHC at present. Even if one takes EWBG into consideration, we note a second, backup mechanism [57]: ρ_{tc} at $\mathcal{O}(1)$ with near maximal phase can also drive EWBG if ρ_{tt} accidentally vanishes in g2HDM. However, it would still make probing $\rho_{tu} \neq 0$ rather challenging, and the LHC experiments would have to try their best at the HL-LHC, as we have tried to illustrate. This is especially so if $\mathcal{B}(B \to \mu\bar{\nu})/\mathcal{B}(B \to \mu\bar{\nu})$ is found by Belle II to differ from SM expectation. On the other hand, baryogenesis may not occur through g2HDM, hence one should exploit the full potential of the LHC.

In summary, we pose the question: "If the flavor chang-

ing neutral Higgs coupling ρ_{tu} is nonzero, how can one check this at the LHC?" With only $\rho_{tu} \neq 0$, we show that it is possible with HL-LHC, by comparing the significance of positively vs negatively charged same-sign dilepton events. Nonzero ρ_{tc} can mimic ρ_{tu}-induced events, while $\rho_{tt} \neq 0$ would further dilute the sensitivity to finite ρ_{tu}. The issue would become important if the ratio of $B \to \mu\bar{\nu}$ decay rate to $B \to \tau\bar{\nu}$ is found by Belle II to deviate from Standard Model expectation.

Acknowledgments.– This work is supported by MOST 106-2112-M-002-015-MY3, and 108-2811-M-002-537 of Taiwan, and NTU 108L104019.

[1] G. Aad *et al.* [ATLAS], Phys. Lett. B **716**, 1 (2012); S. Chatrchyan *et al.* [CMS], *ibid.* B **716**, 30 (2012).
[2] See e.g. G.C. Branco, P.M. Ferreira, L. Lavoura, M.N. Rebelo, M. Sher and J.P. Silva, Phys. Rept. **516**, 1 (2012); and references there in.
[3] S.L. Glashow and S. Weinberg, Phys. Rev. D **15**, 1958 (1977).
[4] W.-S. Hou, Phys. Lett. B **296**, 179 (1992).
[5] K.-F. Chen, W.-S. Hou, C. Kao and M. Kohda, Phys. Lett. B **725**, 378 (2013).
[6] G. Aad *et al.* [ATLAS], JHEP **1406**, 008 (2014).
[7] P.A. Zyla *et al.* [Particle Data Group], to be published in Prog. Theor. Exp. Phys. **2020**, 083C01 (2020).
[8] V. Khachatryan *et al.* [CMS], Phys. Lett. B **749**, 337 (2015).
[9] G. Aad *et al.* [ATLAS and CMS], JHEP **08**, 045 (2016).
[10] A.M. Sirunyan *et al.* [CMS], Eur. Phys. J. C **79**, 421 (2019).
[11] G. Aad *et al.* [ATLAS], Phys. Rev. D **101**, 012002 (2020).
[12] W.-S. Hou and M. Kikuchi, Eur. Phys. Lett. **123**, 11001 (2018).
[13] P. Chang, K.-F. Chen and W.-S. Hou, Prog. Part. Nucl. Phys. **97**, 261 (2017).
[14] See, e.g., S. Davidson and H.E. Haber, Phys. Rev. D **72**, 035004 (2005).
[15] W.-S. Hou, M. Kohda and T. Modak, Phys. Rev. D **99**, 055046 (2019).
[16] W.-S. Hou and T. Modak, Phys. Rev. D **101**, 035007 (2020)
[17] D.K. Ghosh, W.-S. Hou and T. Modak, arXiv:1912.10613 [hep-ph].
[18] M. Aaboud *et al.* [ATLAS], JHEP **1905**, 123 (2019).
[19] A.M. Sirunyan *et al.* [CMS], JHEP **1806**, 102 (2018).
[20] W.-S. Hou, M. Kohda, T. Modak and G.-G. Wong, Phys. Lett. B **800**, 135105 (2020).
[21] E. Kou, P. Urquijo *et al.* [Belle II], PTEP **2019**, 123C01 (2019).
[22] The study of the ρ_{ut}-induced $ug \to tH/tA \to tt\bar{u}$ process can follow a similar strategy.
[23] W.-S. Hou, G.-L. Lin, C.-Y. Ma and C.-P. Yuan, Phys. Lett. B **409**, 344 (1997).
[24] M. Kohda, T. Modak and W.-S. Hou, Phys. Lett. B **776**, 379 (2018).
[25] W.-S. Hou, M. Kohda and T. Modak, Phys. Lett. B **786**, 212 (2018).
[26] W.-S. Hou, M. Kohda and T. Modak, Phys. Lett. B **798**, 134953 (2019).
[27] W. Altmannshofer, J. Eby, S. Gori, M. Lotito, M. Martone and D. Tuckler, Phys. Rev. D **94**, 115032 (2016).
[28] S. Iguro and K. Tobe, Nucl. Phys. B **925**, 560 (2017).
[29] S. Iguro and Y. Omura, JHEP **1805**, 173 (2018).
[30] Q.-H. Cao, S.-L. Chen, Y. Liu and X.-P. Wang, Phys. Rev. D **100**, 055035 (2019).
[31] A.M. Sirunyan *et al.* [CMS], Eur. Phys. J. C **80**, 75 (2020).
[32] A.M. Sirunyan *et al.* [CMS], Eur. Phys. J. C **78**, 140 (2018).
[33] We thank K.-F. Chen for clarifications on this point.
[34] J. Alwall *et al.*, JHEP **1407**, 079 (2014).
[35] R.D. Ball *et al.* [NNPDF], Nucl. Phys. B **877**, 290 (2013).
[36] T. Sjöstrand, S. Mrenna and P. Skands, JHEP **0605**, 026 (2006).
[37] J. Alwall *et al.*, Eur. Phys. J. C **53**, 473 (2008).
[38] J. de Favereau *et al.* [DELPHES 3], JHEP **1402**, 057 (2014).
[39] A. Alloul, N.D. Christensen, C. Degrande, C. Duhr and B. Fuks, Comput. Phys. Commun. **185**, 2250 (2014).
[40] G. Cowan, K. Cranmer, E. Gross and O. Vitells, Eur. Phys. J. C **71**, 1554 (2011).
[41] The ATLAS collaboration, ATLAS-CONF-2020-013.
[42] We digitized the figure of Ref. [41] to obtain the 95% C.L. limit on $\sigma \times \mathcal{B}$, analogous to W.-S. Hou, M. Kohda and T. Modak, Phys. Rev. D **98**, 015002 (2018).
[43] G. Aad *et al.* [ATLAS], JHEP **2006**, 046 (2020).
[44] M. Aaboud *et al.* [ATLAS], JHEP **1812**, 039 (2018).
[45] The ATLAS collaboration, ATLAS-CONF-2016-037.
[46] E. Alvarez, D.A. Faroughy, J.F. Kamenik, R. Morales and A. Szynkman, Nucl. Phys. B **915**, 19 (2017).
[47] A.M. Sirunyan *et al.* [CMS], Eur. Phys. J. C **77**, 578 (2017).
[48] J.M. Campbell and R.K. Ellis, JHEP **1207**, 052 (2012).
[49] SM Higgs production cross sections at $\sqrt{s} = 14$ TeV: `https://twiki.cern.ch/twiki/bin/view/LHCPhysics/CERNYellowReportPageAt14TeV2010`.
[50] J. Campbell, R.K. Ellis and R. Röntsch, Phys. Rev. D **87**, 114006 (2013).
[51] W.-S. Hou, M. Kohda and T. Modak, Phys. Rev. D **96**, 015037 (2017).
[52] ATLAS-CMS recommended $t\bar{t}$ cross section predictions: `https://twiki.cern.ch/twiki/bin/view/LHCPhysics/TtbarNNLO`.
[53] Y. Li and F. Petriello, Phys. Rev. D **86**, 094034 (2012).
[54] A. Crivellin, A. Kokulu, C. Greub, Phys. Rev. D **87**, 094031 (2013).
[55] B. Altunkaynak, W.-S. Hou, C. Kao, M. Kohda, B. McCoy, Phys. Lett. B **751**, 135 (2015).
[56] See the twiki page `https://twiki.org/cgi-bin/view/Sandbox/FlavorChangingNeutralHiggs`.
[57] K. Fuyuto, W.-S. Hou and E. Senaha, Phys. Lett. B **776**, 402 (2018).